Hindawi
Shock and Vibration
Volume 2023, Article ID 4051413, 11 pages
https://doi.org/10.1155/2023/4051413

Research Article

Monitoring Soil-Pile Stripping Damage at Different Temperatures via Piezoelectric Ceramic Sensors

Daopei Zhu,[1] **Xu Liu**,[1] **Zhangli Wang**,[2] **and Xiaoli Cai**[1]

[1]*School of Civil and Surveying & Mapping Engineering, Jiangxi University of Science and Technology, Ganzhou 330013, China*
[2]*Gansu Academy of Building Research (Group) Corporation Limited, Lanzhou 730070, China*

Correspondence should be addressed to Zhangli Wang; zhangli.wang@hotmail.com

Received 8 February 2023; Revised 10 May 2023; Accepted 9 October 2023; Published 30 October 2023

Academic Editor: Vittorio Memmolo

Large temperature differences exist between the winter and summer seasons in different regions of China. Such temperature differences, caused by seasonal changes, may affect the life cycles of piles. Under natural conditions, such as long-term operation under the ambient environment and loads, piles and the surrounding soil undergo peel damage. To study such peel damage between the pile and soil at different temperatures, we installed concrete test piles in soil and subjected them to different temperatures. A crack with a width of 2 cm, depth of 10 cm, and damage range of 90° was applied at the side of the piles. Furthermore, a horizontal impact load was applied near the top of the pile and a piezoelectric ceramic sensor was used to obtain the stress wave response signals. The experimental results reveal that with a decrease in the soil temperature, the amplitude and fluctuation range of the signals received by the piezoelectric sensor decreased. According to the experimental results, in the group with the greatest influence of temperature, keeping other conditions unchanged and setting different crack depths, the horizontal impact load can also be introduced to observe the frequency change. It can be observed that the larger the crack depth, the smaller the frequency. Finally, ABAQUS was used for simulations, whose results were found to be consistent with those of the experiments. This paper describes a method for determining the safety of soil and piles with peel damage at different temperatures, and it also provides a validation of the necessity of holding the rest constant.

1. Introduction

Pile foundations can provide high bearing capacities owing to their uniform and small settlement, excellent compressive strength, pull-out characteristics, seismic performance, and easily mechanized operation, among other features. Consequently, they are widely used for various buildings. A pile foundation performs the function of connecting preceding and following sections during the construction process; hence, it serves to transfer the load borne by the superstructure to the surrounding soil layer smoothly and safely, satisfying the requirements of the vertical deformation limit of the superstructure. Therefore, the interactions between the pile and soil are particularly important and have attracted wide interest. For instance, Abdorazaqi et al. [1] studied the soil-pile interactions in heterogeneous transversely isotropic media, and it is found that under the influence of the heterogeneity of soil medium, the stress transfer process is along the depth of soil layer. Abedzadeh and Pak [2] studied the continuum mechanics of soil-pile lateral interactions using the parallel formula of the Fredholm equation and the singular integral equation and found that not only can more reliable benchmarks be provided for numerical comparisons but also a picture of the clarified underlying physics, as well as a deeper insight into the mathematical properties of the associated boundary value problems. The reasonable mechanics of axial soil-pile interaction studied by Pak and Ji [3] can effectively calculate the distribution of singular joint loads acting on piles. Shahmohamadi et al. [4] investigated the axial soil-pile interactions in a transversely isotropic half space, and it is shown that the present transversely isotropic formulation can analyze the base case of degradation to isotropy. For cold areas where the soil may freeze, Sato et al. [5] studied the influence of surface freezing on the soil-pile

interactions, and the research shows that even when the freezing depth is relatively thin, the stiffness of pile cap will increase significantly during freezing, which indicates that the freezing of foundation has a great influence on the pile-soil interaction. Zhou et al. [6] studied the soil-pile interaction of frozen soil foundations based on changes in the freezing swelling rate and soil stiffness, and it is found that the stress level of frozen soil increases with the increase of frost heave depth, which leads to the increase of frozen soil stiffness and the decrease of the frost heave rate. For areas with more plum rain seasons, Xiao et al. [7] studied the soil-pile interactions in an expansive soil foundation and compared analytical solutions with numerical simulation results, and it was found that with the increase of irrigation amount, the axial displacement and axial tension increased and the sensitivity of these two indices to the incoming water became less and less. Fattah et al. [8, 9] conducted the vertical vibration excitation response test of a single pile in saturated soil and found that the presence of water softened the soil around the pile, reduced the effect of pile side friction, and thus increased the transfer proportion of the pile end load. However, in the dry sandy soil area, Fattah et al. [10–12] found that the pile end load decreases with the change of the burial depth ratio and operation frequency, and for loose and medium relative density soils, the amplitude of acceleration increases with increasing frequency. Because soil has a certain moisture content, changes in temperature will result in variations in the soil's cohesive force. The temperature increases the cohesive force, and the internal friction angle of the soil is reduced; however, increasing temperature has little effect on the bearing capacity of single pile. When the temperature decreases below zero degree Celsius, the ice content of soil increases and freezing occurs, but the compressive strength of pile concrete increases with decreasing temperature [13]. Temperature also affects the shear strength of the soil-pile interface [14], size and ice content of the hardened concrete [15], and performance of the reinforced concrete [16]. Seasonal soil temperature changes and global warming also have significant impacts on the earthquake disasters in permafrost regions [17]. In most regions of the world, seasonal alternation produces a large temperature difference, resulting in a freeze-thaw cycle; this, in turn, affects the nature of the soil and causes a certain degree of damage to the concrete pile, thereby affecting the service life of the pile foundation. Therefore, many scholars have monitored the changes in soil mass and the damage to concrete under freeze-thaw cycles [18–23]. Owing to their small volume, simple manufacturing process, fast frequency response, and high sensitivity, piezoelectric sensors are often used in monitoring processes; they are also widely employed for monitoring crack propagation in cement-based composite materials and closed [24], the initiation and propagation of fatigue cracks in steel bridges [25], and the crack damage in concrete structures [26], among other applications. Jiao et al. reviewed the application of piezoelectric sensing technology in structural health monitoring [27]. Structural health monitoring technology, which can help improve the reliability and safety of important engineering structures, has become an increasingly important research topic with regards to economic maintenance infrastructure [28]. This innovative method has been identified in civil engineering [29]. Embedded sensors are also used to monitor the dynamic mechanics of concrete. Embedded piezoelectric transducers are used to monitor the early strength of concrete [30], whereas embedded piezoelectric ceramic sensors are used to monitor the health of concrete structures [31]; their mechanical sensing performance has also been analyzed [32].

Zhang et al. could quantitatively assess the severity of beam damage by changing the crack depth and hole depth and range on a wood beam and observing the changes in the signal value received by the PZT sensor [33], and the experimental results show that this method is a promising tool for monitoring wood damage in real time. Jiang detected cracks in FRP-reinforced concrete beams based on the embedded piezoelectric ceramic intelligent aggregate [34]; when the damage caused by cracks occurs, the amplitude in the time domain, the amplitude in the frequency domain, and the wavelet packet energy of the signals received by the SA sensor all decrease. Therefore, the active sensing method developed based on piezoelectric ceramics can monitor the occurrence and development of cracks in concrete beams reinforced by FRP in real time. In this paper, based on the previous research, the piezoelectric ceramic sensor is used to monitor the bond state of spalling damaged pile foundation under different temperatures. The pile and soil were exposed to different temperatures, and transverse loads were imposed on the pile using a test hammer. A piezoelectric ceramic sensor embedded in a concrete pile was then used to monitor the stress wave responses of the pile. It is of great significance to use certain test and monitoring technology in pile design and construction under different temperatures to judge and detect whether there is damage in pile foundation.

2. Monitoring Method

Reinforced concrete piles vibrate when they are struck, and different bond states between the concrete pile and surrounding soil result in different stress wave responses. When the ambient temperature around the pile is too low or the soil mass is damaged, the generated energy wave will be lost in the propagation process, resulting in the signal received by the SA sensor falling compared with the signal passing through the pile foundation in healthy state, as shown in Figure 1. To quantitatively assess the severity of the injury, in this study, the energy index of the wave signal was used to measure the bond stiffness between the reinforced concrete pile and clay. Here, X represents a series of discrete signals acquired by the sensor within a given sampling time (0.1 s in this experiment); after sampling, X_i represents the voltage value for the ith time sensor, and E represents the energy index of the wave signal collected within the sampling time and is a scalar that reflects the energy of the wave signals. For a given sampling time, multiple sampling points can be calculated using the following formula:

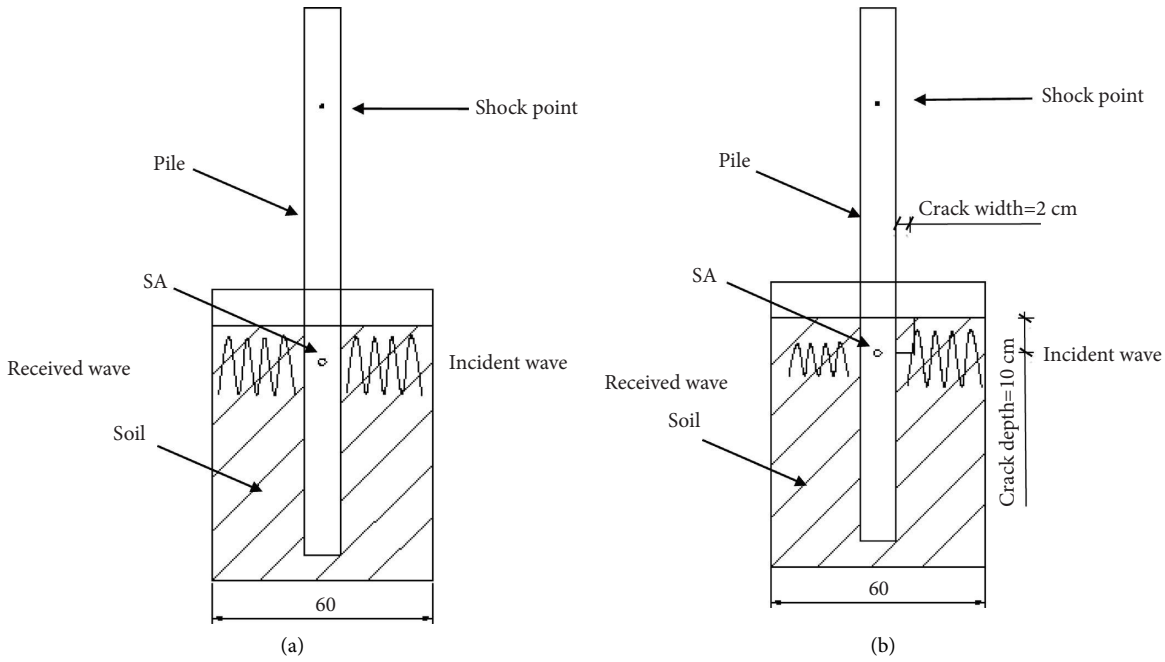

Figure 1: An active sensing method for pile damage detection based on the stress wave. (a) Pile foundation without spalling damage. (b) Pile foundation with spalling damage.

$$X_i = (x_1, \cdots, x_n), \quad (i = 1, 2, \cdots\cdots\cdots), \tag{1}$$

$$E = \|X\|^2 = x_1^2 + x_2^2 + \cdots + x_n^2 = \sum_{i=1}^{n} x_i^2. \tag{2}$$

During temperature changes, the moisture content in the soil varies and the original skeleton and structure of the soil are also altered. When the temperature is less than 0°C, the water between soil particles condenses into ice crystals; thus, the soil around the reinforced concrete pile becomes more restrictive to the pile. Furthermore, a change in the constraint conditions around the reinforced concrete pile affects the value of the energy index.

3. Materials and Instruments

Lead zirconate titanate (PZT) is a solid solution of Pb (Zr, Ti) O_3, composed of $PbTiO_3$ and $PbZrO_3$. Its piezoelectric coefficient is large, its Curie point temperature exceeds 300°C, its mechanical and electrical parameters are not significantly affected by temperature, and its time stability is good. PZT materials with different properties can be obtained by adding one or two trace elements (such as niobium, antimony, tin, manganese, and tungsten) to zirconate titanic acid. Therefore, PZT piezoelectric ceramics are the most widely used piezoelectric materials for piezoelectric sensors. The PZT used in this study was PZT-5; the relevant parameters are listed in Table 1.

The signal acquisition and processing analyzer can collect wave signals from low to high frequencies with a high acquisition accuracy; it can provide comprehensive analysis results, including the amplitude, time domain, frequency domain, and other aspects of various analysis methods.

4. Experimental Setup and Steps

4.1. Experimental Setup. A 1000 mm × 600 mm × 800 mm refrigerator was prepared in advance. The silty clay with a density of 1391 kg/m^3 measured by ring tool method was selected as the experimental soil. The ring tool method is to use a ring tool with known mass and volume to cut soil samples. After weighing and subtracting the mass of the ring tool, the mass of the soil is obtained. The volume of the ring tool is the volume of the soil and then the density of the soil can be obtained. First, piezoelectric plates and concrete were used to prepare the intelligent aggregate; subsequently, wires were used to connect the intelligent aggregate with the BNC joint (Figure 2). In this study, the dimensions of the piezoelectric intelligent aggregate (SA) were 20 mm × 15 mm × 16 mm. The PZT sheet was connected to the wire and then buried between the two concrete blocks. Finally, the groove was filled with epoxy resin for sealing (Figure 3). The dimensions of the PZT plate were 10 mm × 10 mm × 0.3 mm, and it converted extremely weak mechanical vibrations into electrical signals. The signal acquisition instrument collected the electrical signals from the SA sensor and reflected the fluctuations in the electrical signals on a computer. The radius of the reinforced concrete pile used in the test was 40 mm, and its length was 1500 mm. The concrete strength grade was C35, elastic modulus (E) was $3e^{10}$ Pa, and Poisson's ratio (ν) was 0.2. Before concrete pouring, the piezoelectric intelligent aggregate was fixed to the reinforcement cage, and the concrete was cured for 28 d after pouring. Finally, the test pile was placed in the

Table 1: PZT-5 parameters.

Relative permittivity	Electromechanical coupling coefficient	Density ($kg \cdot m^{-3}$)	Mechanical quality factor	Piezoelectric constant ($C \cdot N^{-1}$)			Curie temperature (°C)
ε	Kp	ρ	Qm	d15	d31	d33	Tc
1600	60%	7600	80	640×10^{-12}	-150×10^{-12}	400×10^{-12}	360

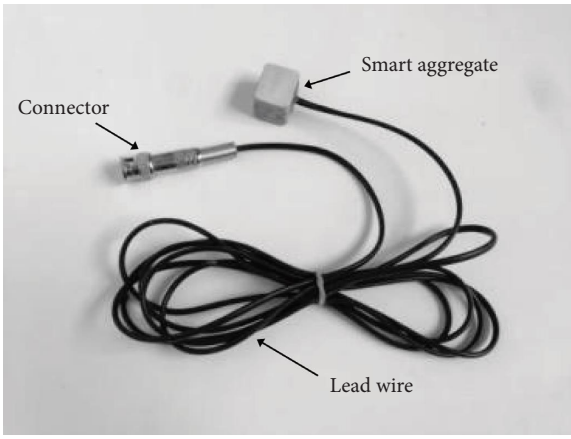

Figure 2: Intelligent aggregates with signal connectors.

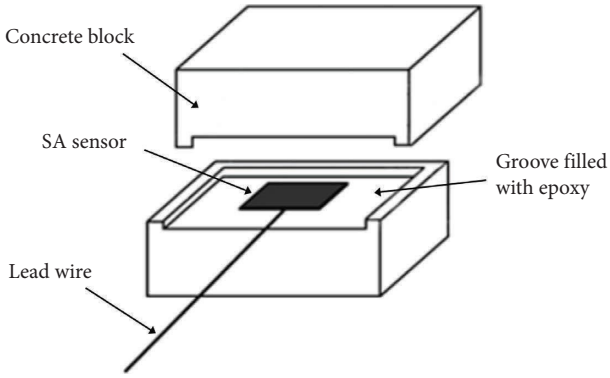

Figure 3: Detailed structure of the intelligent aggregate.

refrigerator. The test device is shown in Figure 4(a). A ruler was attached to the concrete pile (Figure 4(b)); the distance between the ruler and the test pile top is 25 mm, as shown in (Figure 5(a)); its cross-section is shown in Figure 5(b).

Figure 5(b) shows the schematic of the experimental device. The SA sensor was buried 10 cm away from the soil surface, the ruler was set 25 cm away from the top of the test pile, and the position of the small hammer was clearly visible. To apply the same load in each impact, a section of the hammer was suspended from the top of the pile and released from the same height each time.

4.2. Experimental Steps. The bottom of the refrigerator was filled with 5-cm-thick clay; reinforced concrete piles were placed vertically in the middle of the refrigerator. Finally, 65-cm-thick clay was filled. Peel damage was induced on the pile side, with a width of 2 cm, depth of 10 cm, and damage range of 90° (Figure 5). A thin line was fixed at the top of the concrete pile, with the small hammer hanging; thus, the percussion position of the small hammer coincided with the impact point. According to the scale on the ruler, the small hammer was pulled 10 cm away from the reinforced concrete pile and released (Figure 4). When the soil temperature was 30°C, the signal received from the SA sensor was recorded using the signal acquisition instrument and the sampling time was 0.1 s (Figure 6(a)). Subsequently, the contents of the refrigerator were frozen; the temperatures at the end of the freezing process were 10, −5, and −20°C (Table 2). In this manner, the small hammer was released from the same position and the SA signal responses at different temperatures were recorded using a signal acquisition instrument (Figures 6(b)–6(d)).

5. Experimental Results

As shown in Figure 6, under temperatures of 30, 10, −5, and −20°C, the maximum signals amplitudes were 3100, 2700, 2500, and 2200 mV, respectively. With a decrease in temperature, the amplitude and fluctuation range of the electrical signals decreased. This was because the strength of soil increased with a decrease in temperature, and the frost heaving force of soil also increased, resulting in a greater constraint of the soil on the pile. The more constrained the pile, the greater is the energy dissipated from the upper part of the concrete pile in the surrounding soil. In this case, the energy remaining inside the SA sensor decreased; in other words, the amplitude and range of the electrical signal fluctuations from the SA sensor decreased. To quantitatively evaluate the energy attenuation of stress waves, an energy index was used to represent the influence of temperature on the pile peel damage; this energy index was calculated using equations (1) and (2). As shown in Figure 7, the value of the energy index increased with the temperature.

According to the experimental results, the temperature of 30°C electrical signal fluctuation amplitude of the biggest range is the widest. Therefore, we control the soil temperature to 30℃, and keep the width and range of stripping damage unchanged, only the depth of the crack was changed. Then, the vibration frequency of SA signal on the signal acquisition instrument is observed by hitting the concrete test pile with a small hammer. The crack depth is set as 5 cm, 10 cm, 15 cm, and 20 cm, as shown in Table 3 and the schematic diagram of structure is shown in Figure 8.

Figure 9 shows the frequency variation observed at different fracture depths, which is 70 Hz under normal conditions. When the crack depth is 5 cm, the frequency is 65 Hz. When the crack depth is 10 cm, the frequency is 55 Hz. When the crack depth is 15 cm, the frequency is 42 Hz. When the crack depth is 20 cm, the frequency is 32 Hz. With the increase of fracture depth, the frequency decreases obviously. It can be seen that the crack depth will have an impact on the natural frequency of pile foundation and also on the stability and service life of pile foundation. Here, we only set the variation of observation frequency at different crack depths for the temperature that has the greatest impact on peel damage studied above and different temperatures will have different effects.

6. Numerical Verification

To verify the accuracy of the experimental results, we established a finite element model using ABAQUS to further analyze the influence of temperature on the bonding state of the soil-pile system with open peel damage. Based on the

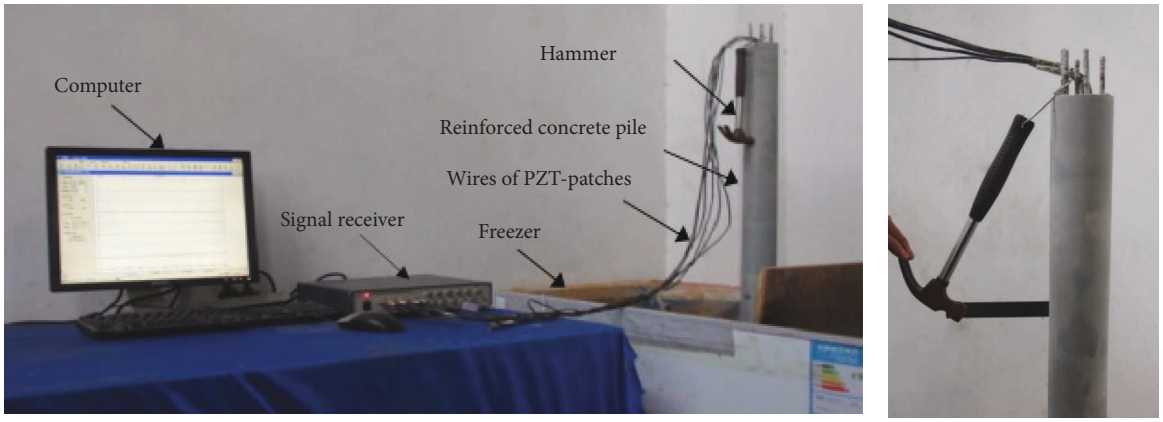

Figure 4: Experimental setup. (a) Test device. (b) A small hammer and a ruler.

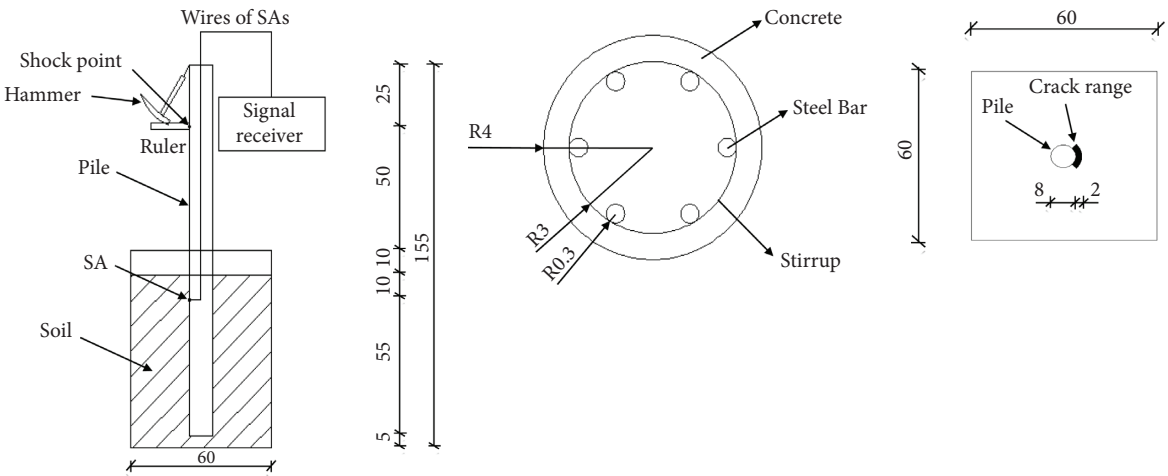

Figure 5: Schematic of the test device and crack setting (unit: cm). (a) Schematic of the experimental device. (b) Cross-section of the concrete pile. (c) Pile side-peeling damage.

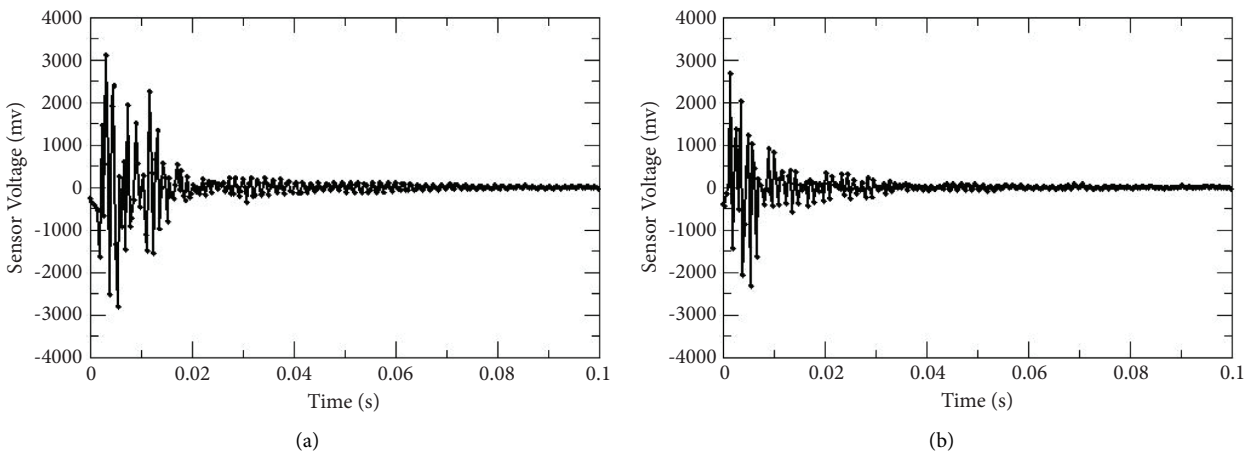

Figure 6: Continued.

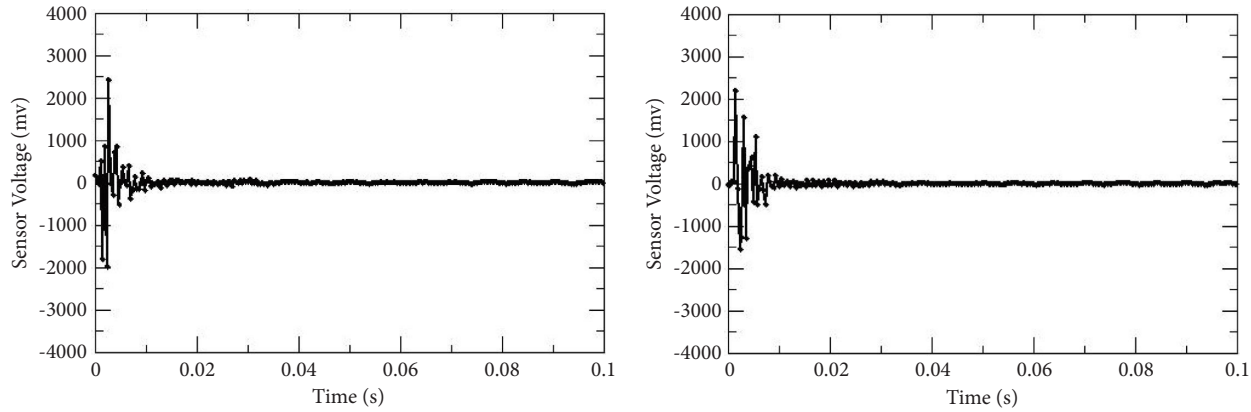

Figure 6: SA signals of soils at different temperatures. (a) Temperature = 30°C. (b) Temperature = 10°C. (c) Temperature = −5°C. (d) Temperature = −20°C.

Table 2: Temperature test case.

Case	1	2	3	4
Temperature	30°C	10°C	−5°C	−20°C
Crack width (cm)	2			
Crack depth (cm)	10			
Crack range (°)	90			

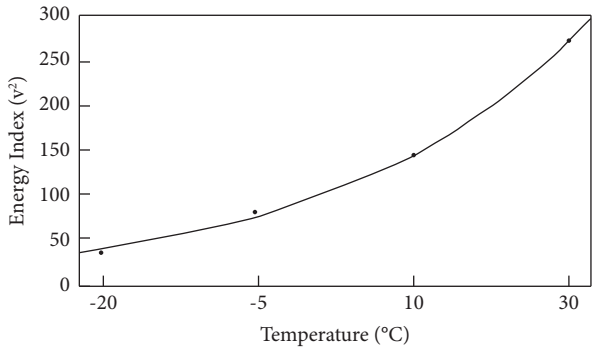

Figure 7: Energy index at different temperatures.

Table 3: Crack depth test cases.

Case	1	2	3	4
Crack depth (cm)	5	10	15	20
Crack width (cm)	2			
Temperature	30°C			
Crack range (°)	90			

component and assembly modeling, users can build and assemble different components according to the problem to be analyzed. As shown in Figure 10, the model was divided into the soil and pile; the dimensions of the soil were set as 60 cm × 45 cm × 70 cm, and its density was 1391 kg/m^3. Moreover, the width, depth, and damage range of the peel damage were set as 2 cm, 10 cm, and 90°, respectively, for the soil model. The pile height was 150 cm; diameter was 8 cm, elastic modulus and Poisson's ratio were 30 GPa and 0.2, respectively, and the strength grade of the concrete was C35.

When using ABAQUS for verification via numerical simulations, heat parameters for the concrete pile and experimental soil should be set considering the simulations at different temperatures. The composition of soils is complex; therefore, certain values are approximated when setting these parameters. The thermal conductivity coefficient of the experimental soil was set as 2.5 W/(m·°C), and the linear expansion coefficient was set as 0.5×10^{-6}/°C. Because the soil used in the experiment was dry soil, the specific heat of the experimental soil was 870 J/(kg·°C), the heat conduction coefficient of the concrete pile was 1.28 W/(m·°C), and the linear expansion coefficient was 9.5×10^{-6}/°C.

Using the method of transient impact response monitoring based on an intelligent aggregate sensor, by varying the temperature of the refrigerator, the experimental soil was set at 30, 10, −5, and −20°C, respectively. The transverse stress distribution of the soil and concrete pile thus obtained is shown in Figure 11. According to the overall stress data, the stress of the soil and concrete piles decreased (increased) with the decrease of temperature, while the crack length, crack width, and crack range of the peel damage remained unchanged. As shown in Figure 11, the stress of the soil near the concrete pile in the middle part was large, and as the temperature decreases, the stress range becomes larger and larger. The stresses on the left and right sides of the soil were small, and the range of the stress decreased with temperature. However, the stress of soil with peeling damage decreases with the decrease of temperature. According to the stress distribution on the concrete pile, the maximum stress was observed at the position where the SA sensor was buried. As the temperature decreased, the stress continued to decrease, indicating that the voltage received by the SA sensor was smaller and that the amplitude and range of the electrical signal fluctuation were increasingly smaller. Thus, this

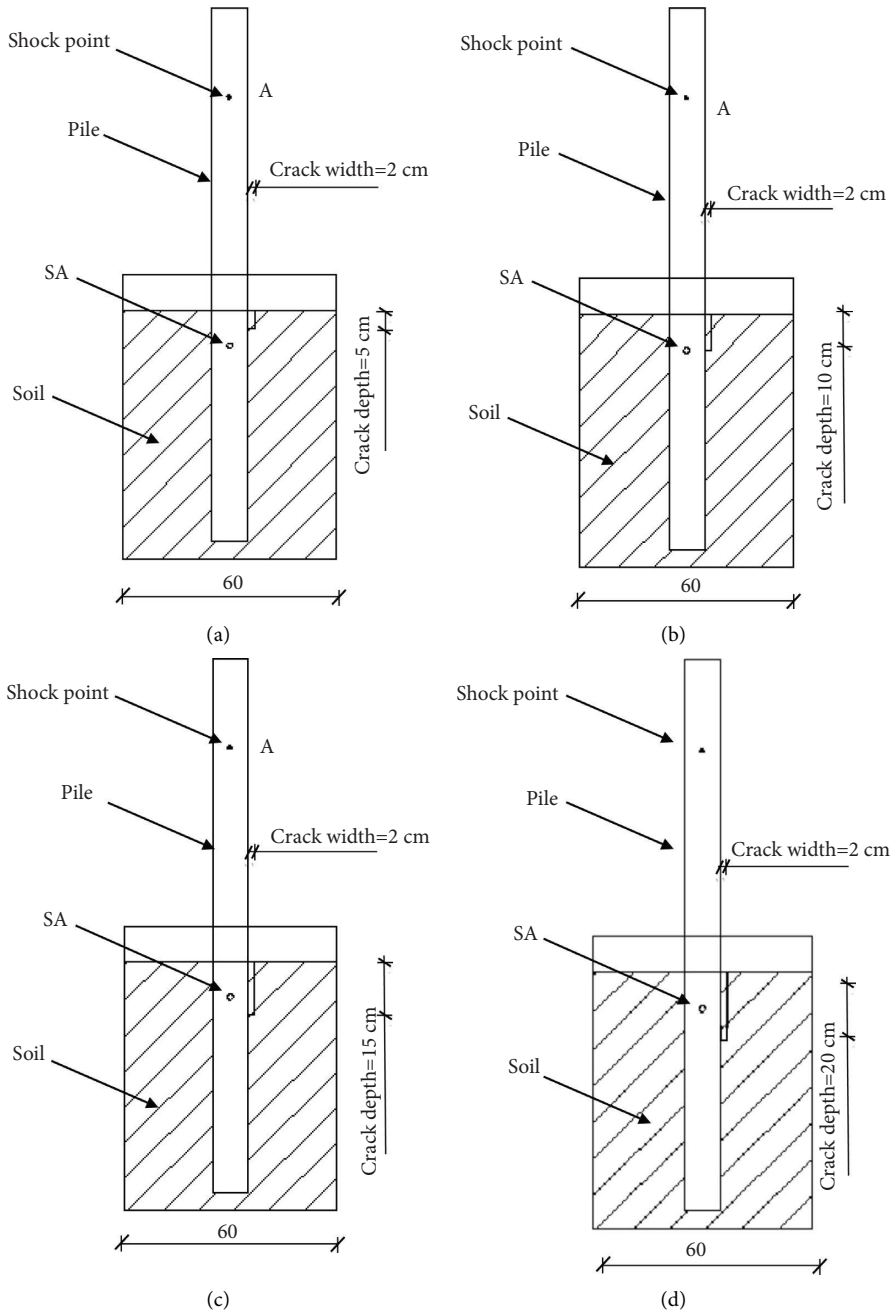

Figure 8: Schematic diagram of the structure with different crack depths. (a) Crack depth = 5 cm. (b) Crack depth = 10 cm. (c) Crack depth = 15 cm. (d) Crack depth = 20 cm.

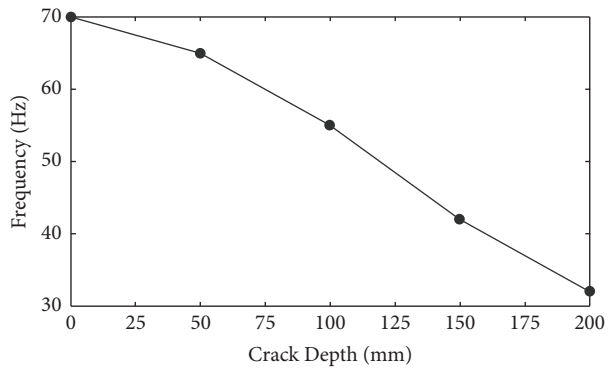

Figure 9: Frequency at different fracture depths.

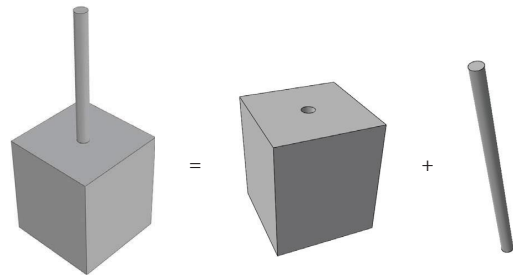

Figure 10: Schematic of the soil and column model.

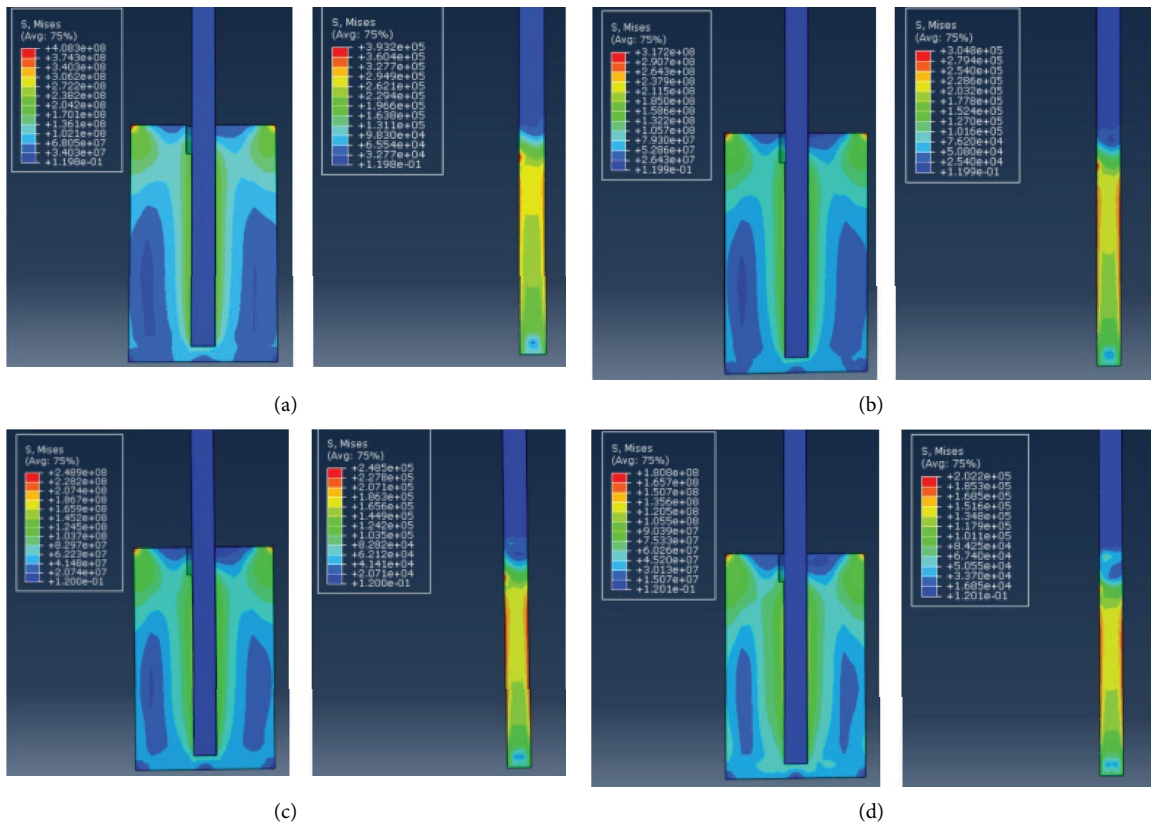

Figure 11: Temperature-stress results (unit: pa). (a) Temperature = 30°C. (b) Temperature = 10°C. (c) Temperature = −5°C. (d) Temperature = −20°C.

method can effectively monitor the bonding state of the soil and piles with peel damage at different temperatures.

7. Conclusion

With a decrease in soil temperature, the amplitude and fluctuation range of the signals received from the piezoelectric sensor decrease. Furthermore, the numerical simulation results were consistent with the experimental ones. The method can provide warnings of the damage to piles in real time according to the data obtained and thus help monitor the health of piles subjected to different temperatures. However, many natural conditions were neglected in this experiment, such as air humidity, soil moisture content in different regions, and soil quality in the southern and northern regions; these aspects will be addressed in future research.

Data Availability

The experimental data used to support the findings of this study are included within the article.

Conflicts of Interest

The authors declare that there are no conflicts of interest.

Acknowledgments

The authors acknowledge the financial support from the Natural Science Foundation of Jiangxi Province, China (no. 20232BAB214074) and the Science and Technology Project of Gansu Provincial Department of Housing and Urban-Rural Development (grant no. JK2023-26).

References

[1] H. Abdorazaqi, A. Khojasteh, M. Rahimian, R. Y. S. Pak, and M. Shahmohamadi, "Soil-pile interaction in inhomogeneous transversely isotropic media," *Soils and Foundations*, vol. 59, no. 3, pp. 738–749, 2019.

[2] F. Abedzadeh and R. Y. S. Pak, "Continuum mechanics of lateral soil-pile interaction," *Journal of Engineering Mechanics*, vol. 130, no. 11, pp. 1309–1318, 2004.

[3] Y. S. Pak and F. Ji, "Rational mechanics of axial soil-pile interaction," *Journal of Engineering Mechanics*, vol. 119, no. 4, pp. 813–832, 1993.

[4] M. Shahmohamadi, A. Khojasteh, M. Rahimian, and R. Y. S. Pak, "Axial soil-pile interaction in a transversely isotropic half-space," *International Journal of Engineering Science*, vol. 49, no. 9, pp. 934–949, 2011.

[5] T. Sato, K. Konagai, T. Ikeda, and H. Nishi, "Effect of surface layer freeze to soil-pile interaction," *MATEC Web of Conferences*, vol. 265, 2019.

[6] Y. L. Zhou, X. Wang, D. R. Liu, F. He, and F. J. Niu, "Pile-soil interactions in frozen soil foundations based on frost heave rate and soil stiffness variations," *IOP Conference Series: Earth and Environmental Science*, vol. 570, no. 2, Article ID 22035, 2020.

[7] H. B. Xiao, C. S. Zhang, Y. H. Wang, Z. H. Fan, and Z. H. Fan, "Pile-soil interaction in expansive soil foundation analytical solution and numerical simulation," *International Journal of Geomechanics*, vol. 11, no. 3, pp. 159–166, 2011.

[8] M. Y. Fattah, B. S. Zbar, and F. S. Mustafa, "Effect of soil saturation on load transfer in a pile excited by pure vertical vibration," *Proceedings of the Institution of Civil Engineers – Structures and Buildings*, vol. 174, no. 2, pp. 132–144, 2021.

[9] M. Y. Fattah, B. S. Zabar, and F. S. Mustafa, "Effect of saturation on response of a single pile embedded in saturated sandy soil to vertical vibration," *European Journal of Environmental and Civil Engineering*, vol. 24, no. 3, pp. 381–400, 2017.

[10] M. Y. Fattah, B. S. Zbar, and F. S. Mustafa, "Vertical vibration capacity of a single pile in dry sand," *Marine Georesources and Geotechnology*, vol. 35, no. 8, pp. 1111–1120, 2017.

[11] M. Y. Fattah, H. H. Karim, and M. K. Mohsen, "Dynamic behavior of pile group model in two layer sandy soil subjected to lateral earthquake excitation," *Global Journal of Engineering Science and Research Management*, vol. 3, no. 8, pp. 57–80, 2016.

[12] M. Y. Fattah, H. H. Karim, and M. K. M. Al-Recaby, "Investigation of the end bearing load in pile group model in dry soil under horizontal excitation," *Acta Geotechnica Slovenica*, vol. 18, no. 1, pp. 79–106, 2021.

[13] X. X. Wang, C. Liu, S. G. Liu, C. W. Yan, J. Zhang, and H. Li, "Compressive strength of pile foundation concrete in permafrost environment in China," *Construction and Building Materials*, vol. 247, Article ID 118431, 2020.

[14] S. Yazdani, S. Helwany, and G. Olgun, "Influence of temperature on soil-pile interface shear strength," *Geomechanics for Energy and the Environment*, vol. 18, pp. 69–78, 2019.

[15] B. Johannesson, "Dimensional and ice content changes of hardened concrete at different freezing and thawing temperatures," *Cement and Concrete Composites*, vol. 32, no. 1, pp. 73–83, 2010.

[16] L. Dahmani, A. Khenane, and S. Kaci, "Behavior of the reinforced concrete at cryogenic temperatures," *Cryogenics*, vol. 47, no. 9-10, pp. 517–525, 2007.

[17] J. Park, O. Kwon, and L. Di Sarno, "Influence of seasonal soil temperature variation and global warming on the seismic response of frozen soils in permafrost regions," *Earthquake Engineering and Structural Dynamics*, vol. 50, no. 14, pp. 3855–3871, 2021.

[18] K. Ma, J. G. Hou, and J. Y. Jia, "Research on the process of concrete damage under frost action," *Advanced Materials Research*, vol. 163-167, pp. 3406–3410, 2010.

[19] W. L. Song, X. F. Li, and K. F. Ma, "The effect of freeze-thaw cycles on mechanical properties of concrete," *Advanced Materials Research*, vol. 163-167, pp. 3429–3432, 2010.

[20] Q. Z. Kong, R. L. Wang, G. B. Song, Z. J. Yang, and B. Still, "Monitoring the soil freeze-thaw process using piezoceramic-based smart aggregate," *Journal of Cold Regions Engineering*, vol. 28, no. 2, Article ID 6014001, 2014.

[21] M. G. Ferrick and L. W. Gatto, "Quantifying the effect of a freeze-thaw cycle on soil erosion: laboratory experiments," *Earth Surface Processes and Landforms*, vol. 30, no. 10, pp. 1305–1326, 2005.

[22] X. Y. Zheng, Y. R. Wang, S. Q. Zhang et al., "Research progress of the thermophysical and mechanical properties of concrete subjected to freeze-thaw cycles," *Construction and Building Materials*, vol. 330, Article ID 127254, 2022.

[23] Y. X. Zheng, L. Yang, P. Guo, and P. Yang, "Fatigue characteristics of prestressed concrete beam under freezing and thawing cycles," *Advances in Civil Engineering*, vol. 2020, no. 12, pp. 1–11, Article ID 8821132, 2020.

[24] H. M. Taha, R. J. Ball, A. Heath, and K. Paine, "Crack growth and closure in cementitious composites: monitoring using piezoceramic sensors," *Sensors and Actuators A: Physical*, vol. 333, Article ID 113221, 2022.

[25] S. Morichika, H. Sekiya, O. Maruyama, S. Hirano, and C. Miki, "Fatigue crack detection using a piezoelectric ceramic sensor," *Welding in the World*, vol. 64, no. 1, pp. 141–149, 2020.

[26] H. Zhang, "The monitoring method for crack damage of concrete structures based on piezoceramics transducers," *Applied Mechanics and Materials*, vol. 578-579, pp. 1134–1137, 2014.

[27] P. C. Jiao, K. J. I. Egbe, Y. W. Xie, A. Matin Nazar, and A. H. Alavi, "Piezoelectric sensing techniques in structural health monitoring: a state-of-the-art review," *Sensors*, vol. 20, no. 13, Article ID 3730, 2020.

[28] H. C. Song and N. Yusa, "A detection sensitivity analysis model for structural health monitoring to inspect wall thinning considering random sensor location," *Research in Nondestructive Evaluation*, vol. 32, no. 2, pp. 74–87, 2021.

[29] S. Alla and S. S. Asadi, "Integrated methodology of structural health monitoring for civil structures," *Materials Today: Proceedings*, vol. 27, no. Pt 2, pp. 1066–1072, 2020.

[30] H. Gu, G. Song, H. Dhonde, Y. L. Mo, and S. Yan, "Concrete early-age strength monitoring using embedded piezoelectric transducers," *Smart Materials and Structures*, vol. 15, no. 6, pp. 1837–1845, 2006.

[31] G. Song, H. Gu, Y. L. Mo, T. T. C. Hsu, and H. Dhonde, "Concrete structural health monitoring using embedded

piezoceramic transducers," *Smart Materials and Structures*, vol. 16, no. 4, pp. 959–968, 2007.

[32] F. Sha, D. Y. Xu, X. Cheng, and S. F. Huang, "Mechanical sensing properties of embedded smart piezoelectric sensor for structural health monitoring of concrete," *Research in Nondestructive Evaluation*, vol. 32, no. 2, pp. 88–112, 2021.

[33] J. C. Zhang, Y. S. Huang, and Y. Zheng, "A feasibility study on timber damage detection using piezoceramic-transducer-enabled active sensing," *Sensors*, vol. 18, no. 5, Article ID 1563, 2018.

[34] T. Y. Jiang, Y. Hong, J. B. Zheng, L. Wang, and H. C. Gu, "Crack detection of FRP-reinforced concrete beam using embedded piezoceramic smart aggregates," *Sensors*, vol. 19, no. 9, Article ID 1979, 2019.